Flow Visualization Through and Around Simplified Models of Biological Structures

Matt Petty

Abstract The morphology of an organism is a key factor in how well it performs a given task. The performance of a certain morphology may change radically under different environmental conditions. To gain an understanding of the interaction between a form and the fluid flowing past it, scale models can be built and several techniques for flow visualization employed. This study examines scale filtering arrays, constructed of flexible or stiff materials, under a range of conditions using a flow tank and 35mm camera. Leakiness, or how restrictive a filtering array behaves, is calculated for each test condition. The arrays protrude from a base plate, which our results indicate has the greatest effect on the flow characteristics through an array.

Introduction

An organism's morphology can greatly affect its ability to perform a certain function such as feeding, collecting sensory input, or locomotion. A particular structure might perform quite differently over a range of environmental conditions. Examining aquatic filter-feeding arrays, Shimeta and Koehl (1997) observed that worms retain different size food particles at different flow velocities and capture differently sized particles over their lifetimes as body size increases. Similarly, a single organism can save energy by passively feeding when currents are favorable, or create favorable currents by moving their appendages in still water (Young and Braithwaite, 1980).

Scaling the size of a structure up or down can also have profound effects on a structure's performance. For example, as a barnacle's feeding appendage increases in size it will theoretically capture more food particles, but at some upper limit will fail mechanically due to hydrodynamic forces (Li and Denny, 2004). In the case of scaling down, a barnacle larva's microscopic feeding appendage might be ineffective due to the unique mechanics of flow around small objects. The barnacle could become perfectly suited to the same task as the appendage increases in size over its life history or when the barnacle makes the transition from a free-floating to a sessile lifestyle.

Considering how an organism interacts with its fluid environment from a mechanistic perspective is a valuable exercise. Understanding the nature of flow past an appendage is fundamental to understanding its function and can lend insight to other fields such as evolutionary biology, animal behavior, and ecology (Koehl, 1998). Reynolds number (Re) is an informative parameter used in fluid dynamics that represents the relative importance of inertial to viscous forces for a particular system. In the equation below U is the velocity of fluid flowing past a form, L is a dimension of the form and ν is the kinematic viscosity of the fluid (Vogel, 1994).

$$Re = \frac{U\,L}{\nu}$$

L is a measure that is applicable over a range of similar forms. For example; if we were comparing a range of airplane wings L could be the wing span, chord or thickness. L can also be arranged so that it is a relationship between a number of measures rather than just a single measure.

Systems with high Re tend to have turbulent flows whereas low Re systems have laminar (or smooth, unidirectional) flows. Also, in low Re systems, the fluid adjacent to an object in a flow may not move in relation to the object, instead it adheres to that object's surface forming a boundary layer. This layer is actually a velocity gradient where flows near an object are slowest and as the distance from the object increases the fluid velocity approaches the free-stream velocity. Small organisms living in low Re environments can be subject to velocity gradients many times their own size, in effect leaving them trapped in a slow-flow zone within their flowing environment (Koehl, 1981).

Objects of the same geometric form, but different scale, will experience the same flow patterns if their Re values are the same. Understanding this relationship allows for scaling study subjects so that modeling and testing of very small or large structures can be performed in the laboratory (Koehl, 2003). Maritime hull testing, for example, employs a model ship scaled to fit the flow apparatus being used, which in most cases would not accommodate a real vessel. To compensate for the reduced size, velocity is increased to achieve the same Re as a full-sized ship would experience under normal operating conditions. This same concept may be applied to microscopic biological structures that are too small to reasonably assess flow patterns around in the laboratory. Reducing velocity and/or increasing viscosity allows for using easily manipulated, larger than life models. The performance of different morphologies can also be tested by scaling the individual elements of a model up or down in relation to one another. Flow around small forms, at low Re, is of particular interest because much of what is assumed about the hydrodynamic function of small biological structures is taken from the study of larger structures and from the human perspective accustomed to life at high Re (Purcell, 1977).

A range of controlled laboratory techniques enables visualization of fluid-flow in relation to an object. Moving scale models through a tank of fluid and recording still images of the flow, as shown by tracer particles suspended in the fluid, is the basic method we chose for this exercise in flow visualization (Loudon and Koehl, 1994).

Organisms use tiny hair-bearing appendages for a wide variety of tasks including particle capture on gill, olfactory and feeding structures. Insect's wings and marine organism's swimming appendages are also often composed of bristled arrays (Koehl, 2004). Our models, designed to represent a bristled structure, are comb-like arrays with multiple repeating "hair" elements running perpendicular to a base at regular intervals. Ultimately, model design is only

limited by construction techniques and imagination, but for preliminary models we chose to use very simple representations to better understand the system in question on a fundamental level. Layers of complexity can be added to the basic design in a stepwise fashion to isolate morphological characteristics such as hair flexibility, taper, spacing and curvature.

This study focuses on the performance of these bristled array morphologies, as measured by leakiness, in order to better understand the biomechanical basis for their form and function. Leakiness is a dimensionless ratio representing how much fluid passes through a restriction, such as the gap between two hairs, compared to how much fluid would have flowed through the same space without the restriction (Loudon and Koehl, 1994). A leaky bristled appendage can act like a sieve, allowing fluid to pass freely while the hairs capture particles. An appendage that isn't leaky will act more like a paddle and can be used for propulsion or to move fluid for other tasks (Cheer and Koehl, 1987). Cheer and Koehl (1987) make mathematical predictions for leakiness through comb-like cylinder arrays. Based on their predictions, large fast moving arrays (high Re) should be leaky and small slow moving arrays (low Re) should act as paddles. These simulations assume rigid cylinders of infinite length with no base or end. The models employed in this study incorporate cylinders of finite length protruding from a base plate representing the body surface to which the appendage would be attached. Our first hypothesis is that leakiness will increase as a function of distance from the base plate. This effect should also be less pronounced as Re is increased. We expect these results because the base plate should experience a zone of slow flow near its surface, reducing the leakiness of the cylinders near the plate. To better represent small biological structures, the models designed for this study also employ flexible cylinders. Our second hypothesis is that arrays of stiff cylinders will be more leaky than arrays of flexible cylinders. We expect stiff cylinders that remain perpendicular to the direction of flow will allow more fluid through the array than will flexible cylinders that lie down and deflect flow up and over the array.

Methods

Scale models of feeding structures are towed through a tank of fluid containing tracer particles. A camera follows the model over the course of a test run recording in a flow field image the model's position relative to the tracer particles. Multiple frames are recorded at even intervals during a single test run. Tracking the position of a single particle over two consecutive

frames yields a vector representing flow. These observed flow vectors are then compared to the potential flow to calculate the model's leakiness for a given flow scenario.

Tow-tank and models The tow-tank, 1 x 0.5 x 0.5 m (L x W x H), is made of 22 mm clear Plexiglas sheet and fitted with a drain to facilitate fluid changes. For the Re scenarios required in this study the tank is filled with thick corn syrup. Small bubbles are formed during pumping that last indefinitely. These bubbles act as tracer particles allowing the movement of fluid to be photographed. Corn syrup is ideal because the tracer bubbles are held immobile and there is very slight movement due to convection. Using the Reynolds number calculation noted above, models and test velocities are scaled to account for using corn syrup instead of water and still be able to model the biological conditions in question.

At the open top of the tank, along either long side, screw-fed linear slides are mounted to drive the camera and model. A computer-controlled stepper motor, capable of precise acceleration and velocity, drives the slides at constant run speeds. Re is varied using different run velocities and holding viscosity and element diameter constant. A model and camera support bridges the two slides perpendicular to the length of the tank and the direction of motion. The models consist of four cylindrical elements (10cm long, 2mm diameter), evenly spaced in a line, protruding from a clear Plexiglas base plate. This can be visualized as a fork poked through cardboard. Flexibility is varied using stainless spring steel (stiff) and nylon (flexible) elements The models hang with the base plate on the surface of the corn syrup with the elements protruding down vertically, at a right angle to the direction of travel.

Camera and lighting Precise cross sections are recorded using selective lighting and focus. A 35mm digital camera is attached above, and looking down on, the models, end-on to the cylinder elements. Looking through the clear base plate, the camera can be focused along the length of the elements at varying distance from the base. The beam of a stroboscopic lamp is tuned so that it is a plane parallel to, and coinciding with, the plane of focus of the camera. This 1cm thick light sheet illuminates tracer particles in a controlled cross-section that can be moved the desired distance from the base plate: 1cm (close), 5cm (middle) and 10cm (far). All particles falling outside of this light sheet are not recorded by the camera allowing for strict isolation of particles at a certain depth from the base plate.

Test-runs A run begins with dimming the lights in the studio, triggering the motor to begin movement and waiting for the models to reach a steady state. Steady state is defined as when the

model is traveling at a constant velocity and the model elements are fully flexed. Upon reaching steady state, the camera is triggered to record ten evenly timed images. The resulting images are downloaded to a computer and catalogued. Using image analysis software (ImageJ), individual particle's positions are noted, by human eye, from one frame to the next. Because the different particle's apparent color and size varies due to their position in the light sheet it is quite easy to track a particle over multiple frames. Also, identification is aided by a particle's tendency to move in a predictable manner over the time sequence. These starting and ending positions, coupled with the time interval between images allows for vectors to be created representing actual flow. Comparing the area described by the total actual flow to the area swept by the array over the same time period yields leakiness.

Results

Leakiness remained constant between the stiff and flexible cylinders at a given depth (Figure 1). The white circles indicate the actual cross-sections of the flexed cylinders while the grey circles represent where the cylinders would be un-flexed. Notice the greater flexibility in the nylon cylinders. The box indicates the total swept area during a run. The area described by the humped scatters and the left edge of the box represent the actual amount of fluid that passed through the cylinders.
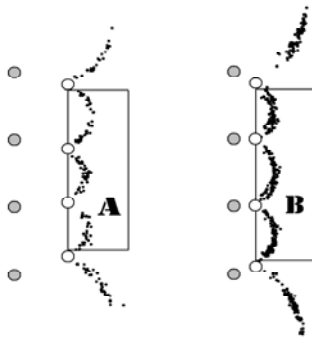

Figure 1- Visual comparison of leakiness between flexible nylon (A) and stiff steel (B) cylinders at 9mm from base. The white circles indicate the actual cross-sections of the flexed cylinders while the grey circles represent where the cylinders would be un-flexed. Notice the greater flexibility in the nylon cylinders. The box indicates the total swept area during a run. The area described by the humped scatters and the left edge of the box represent the actual amount of fluid that passed through the cylinders.

Under all test conditions leakiness increased with distance from the base plate (Table 1).

Table 1- Cylinder Leakiness

Re	Distance from base (mm)	Leakiness (stiff cylinders)	Leakiness (flexible cylinders)
10^{-5} (slow)	1	0.030 ± 0.002	0.051 ± 0.002
10^{-5}	5	0.119 ± 0.004	0.111 ± 0.004
10^{-5}	9	0.213 ± 0.007	0.232 ± 0.008
10^{-4} (fast)	1	0.044 ± 0.001	0.044 ± 0.001
10^{-4}	5	0.092 ± 0.003	0.110 ± 0.004
10^{-4}	9	0.207 ± 0.007	*

*Note: at high speed flexible cylinders deflected out of the 9mm plane of focus

ANOVA results indicate that distance from the base surface is the only significant factor on leakiness ($p < .0001$) while flexibility and Re were not significant ($p = 0.97$ and $p = 0.57$ respectively). Leakiness under the specific conditions of these trials can be predicted by the equation: leakiness $= 0.0138 + 0.0216$(distance in mm). Note that Re and cylinder don't have significant contributions to this model.

Discussion

The most significant effect seen in these trials relates to wall effects on boundary layers. Leakiness tends to decrease as proximity to a wall, in this case the base plate to which the filter arrays are attached, increases. This results from the inherent leakiness of an array being decreased by the slow flow boundary layer's reduced velocity near the base surface. Small animals feeding very close (< 1mm) to the surface on which they are attached may find themselves in a dead zone where little flow is passing through their appendages. To overcome this they may have to fan their appendages to create flow (Young and Braithwaite, 1980). As the animal's size increases and they out-grow the slow flow zones of their adolescence, their behavior might have to change from trying to create flow to having to protect themselves from greater ambient flows. Many marine invertebrates live a free-floating adolescence during their dispersal stage and later attach to a fixed surface. High mortality during dispersal may be due in part to organisms at a small size trapped inside a boundary layer where they encounter very little food particles or are at the mercy of larger bulk-feeding organisms. Issues of community

structure, such as how the spacing between individual organisms and their neighbors, impact the flow through and around each organism.

This study is limited to a two-dimensional view of flow through the test arrays. This may have limited our ability to understand the importance of element flexibility because we were unable to tell whether flow was truly slow in three axes or only appeared to be slow when instead the velocity in the z direction increased. Using two-camera video capture to integrate the three planes of motion in real time would greatly increase the understanding of flow around our arrays and could easily test asymmetric and organic forms.

References

Cheer AYL and Koehl MAR. 1987. Paddles and rakes fluid flow through bristled appendages of small organisms. Journal of Theoretical Biology 129 (1): 17-40

Koehl MAR. 2004. Biomechanics of microscopic appendages: functional shifts caused by changes in speed. Journal of Biomechanics 37 (6) : 789-795

Koehl MAR. 2003. Physical modeling in biomechanics. Philosophical Transactions of the Royal Society of London. 358: 1589-1596

Koehl MAR. 1998. Small-scale hydrodynamics of feeding appendages of marine animals. Oceanography. 11: 10-12

Koehl MAR. 1981. Feeding at low Reynolds number by copepods. Journal of Biomechanics, 14: 486

Li NK and Denny MW. 2004. Limits to phenotypic plasticity: flow effects on barnacle feeding appendages. Biological Bulletin. 206: 121-124

Loudon C, Best BA, Koehl MAR. 1994. When does motion relative to neighboring surfaces alter the flow through an array of hairs? Journal of Experimental Biology. 193:233-254

Merzkirch W. 1996. Flow visualization. Orlando : Academic Press, 266p

Purcell EM. 1977. Life at low Reynolds number. American Journal of Physics. 45:3-11

Shimeta J and Koehl MAR. 1997. Mechanisms of particle selection by tentaculate suspension feeders during encounter, retention and handling. Journal of Experimental Marine Biology and Ecology. 209: 47-73

Vogel S. 1994. Life in moving fluids. Princeton, NJ: Princeton University Press, 484p

Young CM and Braithwaite LF. 1980. Orientation and current-induced flow in the stalked ascidian *Styela montereyensis*. Biological Bulletin. 159: 428-440